Appl. Phys. A 76, 645–652 (2003)
DOI: 10.1007/s00339-002-2003-6

Applied Physics A
Materials Science & Processing

J.V. BARTH[1,✉]
J. WECKESSER[1,2]
N. LIN[2]
A. DMITRIEV[2]
K. KERN[1,2]

Supramolecular architectures and nanostructures at metal surfaces

[1] Institut de Physique des Nanostructures, Ecole Polytechnique Fédérale de Lausanne, 1015 Lausanne, Switzerland
[2] Max-Planck-Institut für Festkörperforschung, 70569 Stuttgart, Germany

Received: 4 June 2002/Accepted: 2 October 2002
Published online: 5 February 2003 •

ABSTRACT The controlled formation of non-covalent bonds (H-bonding, metal–ligand interactions) is the key ingredient for the fabrication of supramolecular architectures and nanostructures. Upon deposition of molecular building blocks at well-defined surfaces, this issue can be directly addressed. Scanning tunneling microscopy observations are presented, which provide insight into the interaction of functional groups on metal substrates at the molecular level. In particular, carboxylic acids were employed: (4-[(pyrid-4-yl-ethynyl)]-benzoic acid (PEBA), 4-[*trans*-2-(pyrid-4-yl-vinyl)]-benzoic acid (PVBA) and trimesic acid (1,3,5-benzenetricarboxylic acid, TMA), which could be stabilized in a flat geometry at the surface. By choosing the appropriate substrate material and symmetry, the sensitive balance of intermolecular and molecule–substrate interactions can be tuned to obtain well-defined supramolecular architectures and nanostructures. The head-to-tail hydrogen bonding of the related rod-like species PEBA and PVBA stabilizes molecular rows on Ag(111). The subtle difference in the molecular geometries is reflected in the lateral ordering: While 2-D islanding is encountered with PEBA, 1-D nanogratings of supramolecular chiral H-bonded twin chains evolve for PVBA. The threefold symmetry of TMA in conjunction with the self-complementarity of its exodentate groups accounts for the formation of H-bonded honeycomb networks on Cu(100) at low temperatures. Metal–ligand interactions were probed with PVBA and TMA at Cu surfaces at ambient temperature. Deprotonation of the carboxyl moiety takes place, which readily interacts with Cu adatoms evaporated from step edges. This leads to a head-to-head pairing of PVBA on Cu(111) and cloverleaf-shaped Cu–TMA coordination compounds on Cu(001).

PACS 68.65.-k; 81.16.Fg; 82.30.Rs; 82.65.+r

1 Introduction

The mastery of the non-covalent bond is the leitmotiv in supramolecular chemistry [1–3]. Over the last decades, intricate arrangements from molecular building blocks have been created by synthetic means. This idea originates from living organisms: Natural supermolecules are abundant in biological systems, where their proper functioning is of crucial importance for life. One of the main strategies in the field is self-assembly, which provides unique routes to obtaining nanoscale supramolecular structures [2–6]. Recent studies, where scanning tunneling microscopy (STM) was predominantly employed as an experimental technique, have revealed that with molecular building blocks at well-defined surfaces, direct insight into non-covalent interactions and self-assembly phenomena can be gained in two dimensions [7–14]. A current challenge in this field appears to be the development of strategies for deliberate positioning of functional molecular species at suitable substrates, a decisive aspect in the search for molecular devices [15, 16].

A promising class of compounds for supramolecular aggregates are molecular species comprising functional groups for hydrogen-bond formation. The H-bond energetics are frequently in a useful range and their directionality facilitates fabrication of highly organized assemblies [17–20]. Corresponding molecules have been investigated at metal surfaces [7, 10, 11, 13] and the results demonstrate that organic species with, for example, moieties for head-to-tail or lateral coupling can be successfully employed. This suggests that species with functional groups providing geometrical (steric) or electronic complementarity can be employed in general.

The concept of metal coordination compounds based on specific metal–ligand interactions was introduced by Werner at the turn of the 20th century [21, 22]. Coordinate bonds may be decisive in molecular recognition and offer an excellent means for the fabrication of complex molecular arrangements at the nanoscale. Accordingly, they represent one of the pillars of supramolecular chemistry [1, 2, 6, 23, 24]. The principles of metal–ligand interactions for interconnecting adsorbed species at surfaces remain to be explored. As a promising step, it has been demonstrated in a recent study that arrays stabilized by coordination bonding can be generated on graphite [25].

We have explored the controlled formation of non-covalent bonds for the fabrication of supramolecular nanostructures at surfaces. In particular, a series of carboxylic acids with different shapes and symmetries has been employed. With these species, we disregard the asymmetry of the carboxylic acid group, which can rotate in the gas phase. At the surface, the hydrogen atom is expected to freely transport from one oxygen atom to the other, similar with hydrogen

✉ Fax: +41-21/693-3604, E-mail: johannes.barth@epfl.ch

transfer processes in related molecular systems [26]. The rod-like molecules 4-[(pyrid-4-yl-ethynyl)] benzoic acid (PEBA) and 4-[*trans*-2-(pyrid-4-yl-vinyl)] benzoic acid (PVBA) have been designed for non-linear optics applications [27–29]. The structure formulae given in Fig. 1a and b show that the differences between the two molecules are minute. Both species are rigid and planar. The identical endgroups, i.e. a carboxylic acid ('head') and a pyridyl moiety ('tail'), are designed to form head-to-tail hydrogen bonds (see Fig. 1d), a feature which is found in PVBA and PEBA crystal structures [27, 28]. The ethynylene bridge of PEBA is substituted by a ethenylene bridge in PVBA leading to a slightly increased length of PEBA with respect to that of PVBA (for free molecules, the projection of the distance of the extremal N and H atoms on the symmetry axis of the pyridyl moiety is 12.8 vs. 12.4 Å, the respective core-to-core distances are 12.8 and 12.5 Å). Upon 2-D confinement, the angled molecular structure of PVBA imposes chirality that is not present in the gas phase. Thus two chiral species exist which are labeled λ and δ PVBA, respectively (see Fig. 1b). By contrast, PEBA is linear and thus the adsorbed molecule remains achiral at a surface. Trimesic acid (TMA) – 1,3,5-benzenetricarboxylic acid $C_6H_3(COOH)_3$ – represents a prototype material for supramolecular self-assembly [30, 31]. As depicted in Fig. 1c, it is a polyfunctional carboxylic acid with threefold symmetry comprising a phenyl ring and three identical carboxyl endgroups in the same plane. TMA is known to assemble in diverse supramolecular structures due to the trigonal exodentate functionality, where the most common motif is a planar honeycomb network structure formed through regular dimerization of carboxyl groups (Fig. 1e). In the 3-D α-polymorph of the TMA crystal structure, these networks interpenetrate, i.e. the approximately 14-Å – diameter holes of the honeycomb lattice are catenated. The tendency of network formation in TMA is frequently employed for fabrication of clathrates (inclusion complexes) [30–33]. Under the conditions applied for the present observations, all molecules employed were bound in a flat geometry, i.e. with the aromatic ring parallel to the surface plane.

2 Experimental

Sample preparation and characterization were conducted under ultra-high vacuum (UHV), providing well-defined conditions on atomically clean substrates. Two UHV systems were employed, equipped with a home-built low-temperature STM [34] and a variable-temperature STM [35] (operational in the range of 40–800 K), respectively, as well as standard facilities for sample preparation and characterization. The single crystal surfaces were prepared by cycles of argon-ion sputtering (500–700 eV, 0.5–6 μ A/cm^2) and subsequent annealing (800–900 K), resulting in large defect-free terraces in the 1000-Å range. The molecules were deposited in UHV by organic molecular-beam epitaxy using conventional Knudsen-cells at background pressures of approximately 5×10^{-10} mbar with sample temperatures in the range 100–450 K.

3 Supramolecular architectures with hydrogen bonding

The formation of superstructures stabilized by hydrogen bonds requires that the lateral intermolecular coupling be well balanced with respect to the molecule–substrate interactions. Experiments with PVBA revealed that this can be accomplished by choosing weakly corrugated noble metal substrates (Ag(111), Au(111)). In contrast, the molecule–substrate interactions may dominate on substrates with higher corrugation and chemical activity, such as Pd(110)

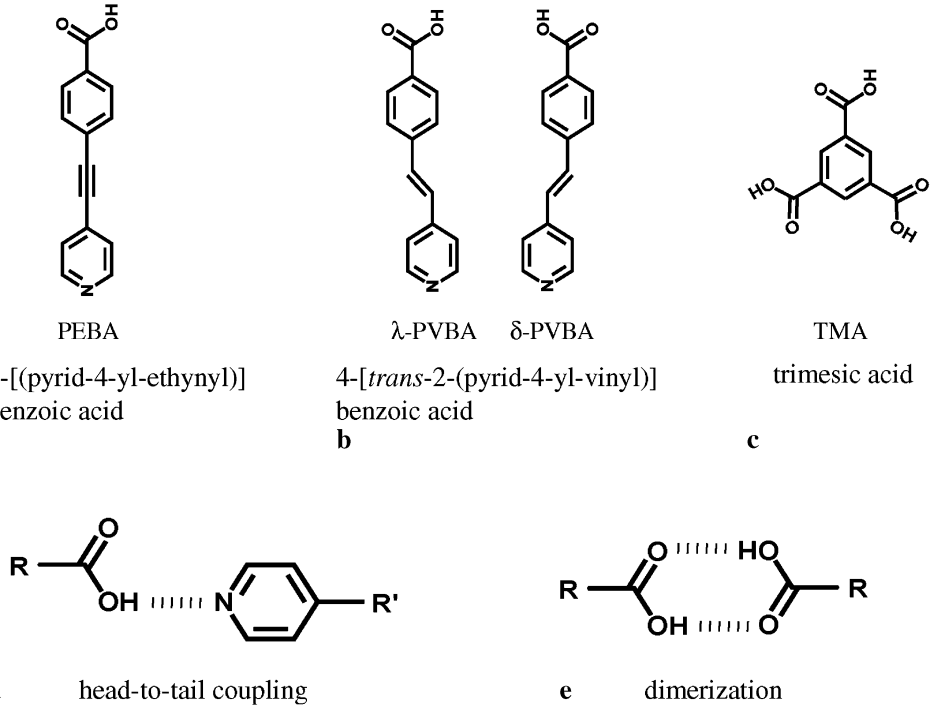

FIGURE 1 The molecular building blocks: **a** 4-[(pyrid-4-yl-ethynyl)] benzoic acid (PEBA); **b** with 4-[*trans*-2-(pyrid-4-yl-vinyl)] benzoic acid (PVBA) two chiral species labeled λ and δ PVBA exist upon 2-D confinement; **c** trimesic acid (TMA) – 1,3,5-benzenetricarboxylic acid $C_6H_3(COOH)_3$; **d** head-to-tail hydrogen bonding between a carboxyl and a pyridyl moiety; and **e** H-bond dimerization of two self-complementary carboxyl groups

and Cu(111), and prevent regular ordering mediated by H-bonding [11, 36, 37].

3.1 *Two-dimensional self-assembly of PEBA on* Ag(111)

Well-ordered structures are formed for PEBA adsorbed on Ag(111) upon annealing low-temperature-grown films or deposition at room temperature. At intermediate coverages, the large terraces are typically nearly saturated, whereas on smaller terraces frequently merely the atomic steps are decorated. In Fig. 2a, the existence of 2-D islands on large terraces is revealed. Within the islands, the head-to-tail coupling feature can be identified. The borders of the islands are usually straight; kinks are energetically unfavorable. This also signals that the mobility of individual molecules along step edges is high when islands evolve. From STM images, the substrate direction of the molecular chains in the different domains and the intermolecular distances were determined. High-resolution data demonstrate that all molecules within the 2-D islands point in the same direction [38]. The supramolecular structure is oriented along $[3\overline{1}\,\overline{2}]$ (in the mirror domains along $[21\overline{3}]$) with a chain periodicity of 15.3 Å and an inter-row distance d of about 6.6 Å [38]. Moreover, detailed data analysis reveals that the molecular axis is slightly rotated ($\sim 5°$) with respect to the superstructure orientation. This effect can be rationalized by the directional nature of the hydrogen bond. In Fig. 2b the proposed model of the PEBA structure is represented. It reveals that the rotation of the molecular axis allows for a better coordination in the head-to-tail coupling between the endgroups and is likely to be supported by the lateral inter-row coupling. The length of the OH · · · N hydrogen bond between PEBA molecules is approximately 2.3 Å (assuming an unrelaxed geometry; the hydrogen–nitrogen distance is given). Theoretical modeling indicates that this configuration is associated with a gain in cohesive energy per molecule of approximately 0.4 eV [38, 39]. The parallel orientation of adjacent PEBA prevents saturation of lateral bonding and thus promotes 2-D growth. It is interesting to note that the islands represent enantiomorphic supramolecular structures due to a distinct shift of neighboring molecular chains in the islands. This is due to the fact that the PEBA molecules do not follow a high-symmetry direction of the substrate. While the threefold substrate symmetry is reflected in three rotational domains on the Ag(111) surface for a given enantiomorphic configuration, the substrate

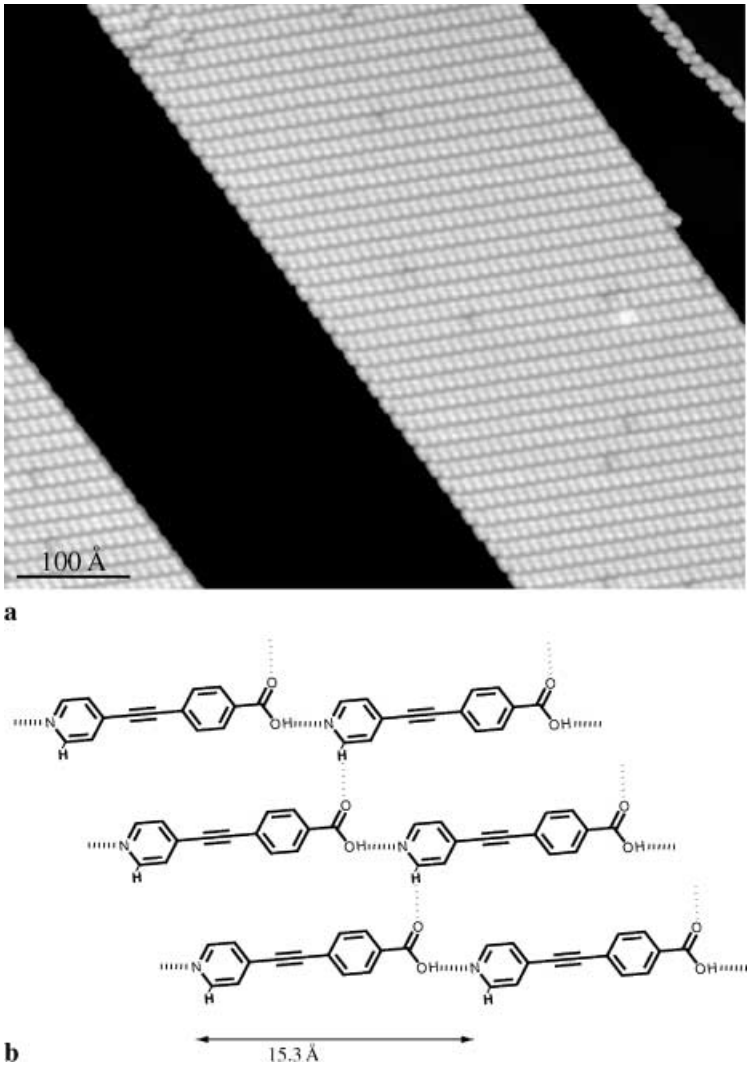

FIGURE 2 **a** STM topograph showing the equilibrium configuration of PEBA on Ag(111) (annealed to 300 K following adsorption at 150 K, measured at 77 K). 2-D islands on large terraces have formed where the PEBA molecules are aligned strictly parallel. The rod-like shape of the flat-lying molecules is clearly visible. The atomic step in the *upper right* is decorated with two PEBA rows. **b** Schematic model for the PEBA supramolecular structure with OH · · · N head-to-tail and weak lateral CH · · · OC hydrogen bonds indicated. For closer proximity of the functional groups and the 2-D interconnection of the rows, the molecular axis is slightly rotated with respect to the orientation of the superstructure. Adapted from [38]

symmetry accounts for a mirror domain to every rotational domain having opposite chirality. Since PEBA is achiral and the molecules in related mirror domains cannot be distinguished, their very packing is at the origin of the enantiomorphic structures encountered here [38].

3.2 *Supramolecular chiral* H-*bonded twin chains in PVBA*/Ag(111)

Extended regular molecular stripe patterns evolve at intermediate PVBA coverages upon equilibration, as demonstrated by the data reproduced in Fig. 3a and b. 1-D aggregates consisting of PVBA twin chains have formed. They run straight along a $\langle 11\overline{2}\rangle$-direction of the Ag lattice and form well-ordered nanogratings at the μm scale [11]. The periodicities of the grating can be tuned by the amount of deposited material or by exploiting dislocation patterns at suitable substrates (e.g. Au(111)) [13, 38]. The twin-chain periodicity is 15 Å, corresponding to $3 \times \sqrt{3}\,a$, where $a = 2.885$ Å is the Ag surface lattice constant). The molecular axes are oriented along the chain direction, in agreement with the expected formation of hydrogen bonds between the PVBA endgroups. Reflecting the threefold symmetry of the Ag(111) substrate, three rotational domains exist on the surface [38]. High-resolution data reveal that within the twin chains, a head-to-tail coupling prevails and that the two molecular rows in a given twin chain are oriented antiparallel [11]. Moreover, the twin chains are enantiomorphic due to the distinct directional shift in the adjacent molecular rows. For example, in the data presented in Fig. 3a it is always the left PVBA row that appears to be displaced in the chain direction. It

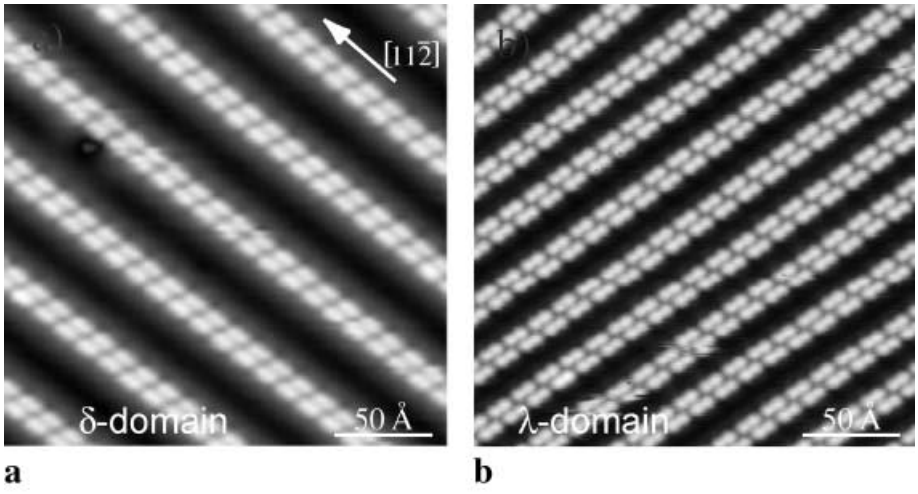

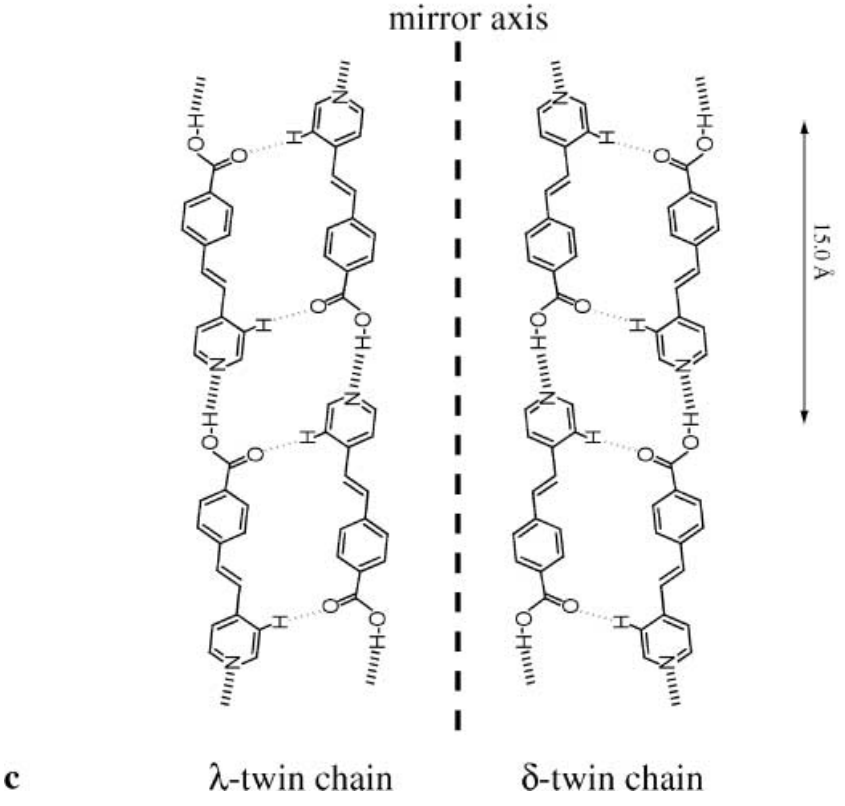

FIGURE 3 Formation of a regular 1-D supramolecular PVBA nanograting by H-bond-mediated self-assembly on the Ag(111) surface at intermediate coverages (following adsorption or annealing at 300 K, measured at 77 K). This pattern is continued in extended domains in the μm-range. The STM images in **a** and **b** reveal that enantiomorphic PVBA twin chains evolve, where the molecular endgroups are connected. Domains exist where the supramolecular chirality of the twin chains is strictly correlated. **c** Schematic model for the two possible supramolecular chiral PVBA twin chains with OH···N and weak lateral CH···OC hydrogen bonds indicated. Adapted from [38]

can be easily seen that the twin chains shown in Fig. 3a cannot be transformed into those shown in Fig. 3b by simple translations and rotations in 2-D. Rather, a mirror operation would be required. Thus, for each rotational domain two possibilities for supramolecular chiral ordering exist. Theoretical modeling indicates that for each type only one chiral PVBA species is employed (Fig. 1b) [13]. Corresponding models are reproduced in Fig. 3c with the hydrogen bonding between the molecules indicated. The OH $\cdots$ N hydrogen bond length is estimated to be 2.5 Å, assuming an unrelaxed molecular geometry. Due to their antiparallel arrangement, the crooked molecules nicely match each other. Furthermore, detailed theoretical analysis reveals that the inward orientation of the more negative double-bonded oxygen atoms simultaneously accounts for lateral bonding and the saturated nature of the repulsively interacting twin chains [13]. A striking feature in the data shown is that all twin chains in the domains shown are of the same chirality (Fig. 3a and b), i.e. there exists a mesoscopic correlation of supramolecular chirality, which was found to be strictly obeyed over the entire μm domains. Consequently, the racemic mixture that had been originally deposited from the stochastic molecular beam underwent spontaneous mesoscopic chiral resolution during the formation of the nanogratings [13].

3.3 *Low-temperature TMA honeycomb phase on* Cu(100)

In Fig. 4a, a STM image revealing hydrogen-bonded TMA assemblies is shown (deposited at 240 K, data recorded at 205 K). The apparent height of the molecules, approximately 1.5 Å, indicates a planar adsorption geometry; this is typical for aromatic molecules with a π-system oriented parallel to the surface [36, 40]. Additional STM data reveal a triangular appearance of the molecules with a characteristic side length of approximately 8 Å [41] (which agrees with the dimensions of an individual TMA molecule [42]). Extended 2-D TMA islands with smooth borders have formed at the surface, decorating the atomic steps. This implies a preferred TMA adsorption at the step edges and an appreciable low-temperature diffusion rate. Within the islands, a honeycomb motif with a periodicity of approximately 20 Å is identified. This configuration is associated with supramolecular self-assembly through dimerization of carboxyl endgroups (Fig. 1e), similar to the network structures in 3-D TMA crystals, as demonstrated by the model depicted in Fig. 4b. When additionally the preference for a specific high-symmetry bonding site at the Cu(100) surface is posed, a slightly increased and deformed cavity of approximately 16×18 Å^2 is suggested [41]. In this case, the characteristic shortest distance between network knots (of ≈ 20 Å) through the center of a single mesh coincides with the corresponding value in the crystal structure of α-polymorph trimesic acid [43]. Assuming an unrelaxed molecular geometry, the average length of the OH $\cdots$ O bond comes close to 2.7 Å (which exceeds by approximately 1 Å the corresponding distance in the crystalline α-phase of TMA [43]). Note that the network formation necessarily implies the free transfer of H atoms from one oxygen atom to the other within the carboxyl groups. In the absence of this effect, the adsorbed flat-lying TMA molecules would exist in several distinct configurations (being partly 2-D chiral), effectively obstructing the periodic dimerization of carboxyl endgroups.

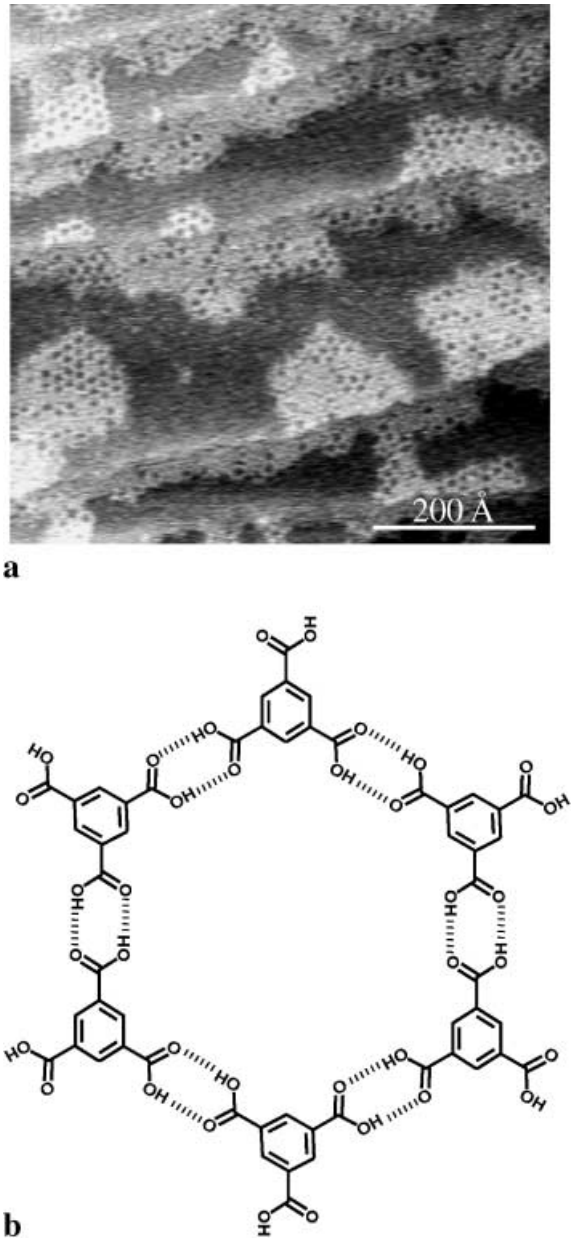

FIGURE 4 **a** STM image of the low-temperature phase of TMA on Cu(100) (deposited at 240 K, image taken at 205 K). In the islands decorating the step edges, a honeycomb motif is resolved, which is associated with extensively hydrogen-bonded 2-D TMA networks. **b** Schematic model for the honeycomb structure with TMA in a flat adsorption geometry and threefold dimerization of self-complementary carboxyl moieties. Adapted from [41]

4 Nanostructuring with metal–ligand interactions

4.1 *Copper–carboxylate bonding in PVBA* / Cu(111)

With the deposition of PVBA on Cu(111) at elevated temperatures ($T = 425$ K), arrangements are encountered which are associated with the formation of copper carboxylates where PVBA molecules are laterally linked via Cu adatoms. The adsorbed molecules are highly mobile at elevated temperatures and in analogy with the surface chem-

istry of related carboxylic acids [44], the PVBA carboxyl moiety is expected to be deprotonated. Simultaneously, mobile Cu adatoms exist within the terraces at the elevated temperature. The reason behind the presence of Cu adatoms is their continuous 2-D evaporation/condensation at atomic step edges, which accounts for the presence of a surface lattice gas. This process can be understood as the 2-D analogue to the coexistence of gas and condensed phases in 3-D systems described by the vapor pressure of a substance. On Cu(111), the atom detachment rate from kink sites onto a terrace is approximately 15 s^{-1} at 425 K [45]. This suggests that lateral interactions between PVBA and substrate adatoms may become important. Upon cooling down, pairs of molecules are preferentially found, as demonstrated by the STM image in Fig. 5a. This pairing is in marked contrast to the repeated head-to-tail motif encountered with PVBA and PEBA on Ag(111). It is associated with lateral copper–carboxylate bonding where two molecules arrange in a linear complex with a flat bonding geometry, as demonstrated by the model in Fig. 5b. Accordingly, the length of the pairs in the STM data amounts to approximately 28 Å. Similar findings have been obtained with benzoic acid and related species on Cu surfaces [44, 46].

4.2 Cu–*TMA compound on* Cu(100)

TMA was observed on Cu(100) at room temperature. Similar to the Cu(111) substrate, a 2-D lattice gas of Cu adatoms was present, leading to a complete deprotonization of the carboxylic groups such that three reactive COO ligands per TMA existed [41, 47]. At appreciable coverages, individual molecules can be resolved as equilateral triangles in STM images (Fig. 6a), reflecting a flat-lying geometry. The symmetry and characteristic side length of approximately 8 Angstrom agrees well with the shape and dimensions of TMA [30, 43]. Four distinct orientations with respect to the substrate lattice were found with one of the triangle corners always pointing along a high-symmetry direction of the Cu(100) surface. This is understood to be as a consequence of high-symmetry site occupation of the aromatic ring at the substrate atomic lattice. The data reveal moreover that the molecules tend to be arranged in a complementary manner, i.e. neighboring TMAs are oriented anti-parallel, which accounts for close packing at the surface due to the space-filling principle. However, this rule is not generally obeyed and arrangements occur where four TMAs form a cloverleaf structure with a bright protrusion at the center. This configuration is associated with a central Cu adatom which is coordinated by the carboxylate ligands from the four surrounding molecules and is hence designated $Cu(TMA)_4$ (The decisive role of atom evaporation from steps could be proven in the present case by the following experiments: On the one hand, evaporation was limited via step decoration by carbon monoxide. In this case, the compound formation was significantly delayed. On the other hand, the compound formation could be triggered by co-deposition of Cu.) A close inspection of the STM image reveals that the TMA carboxylate ligands do not point straight towards the central protrusion in the compound. This demonstrates that the oxygen atoms in the respective COO moieties are not equivalent, indicating a unidentate coordination of the Cu adatom, as illustrated by the model in Fig. 6b.

Assuming an unrelaxed TMA geometry, the Cu–O distance is estimated to be approximately 3 Å, exceeding substantially the characteristic Cu–O distance of approximately 2 Å encountered in 3-D copper carboxylates [48, 49] (note

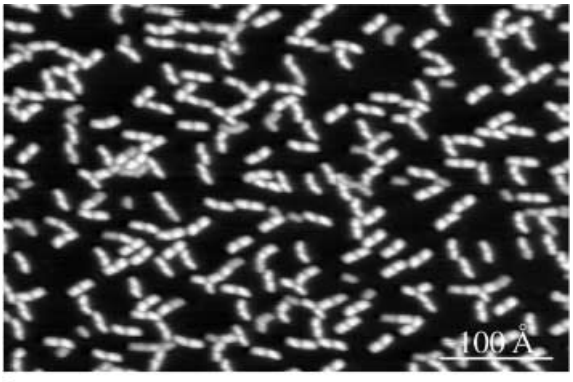

FIGURE 5 **a** Pairing of PVBA molecules upon deposition on Cu(111) at elevated temperatures (adsorption at 425 K, measured at 77 K). The molecules are imaged slightly shorter than on the Ag(111) surface. **b** Model of copper–carboxylate bonding with a head-to-head pairing of two PVBA molecules with deprotonated carboxyl moieties

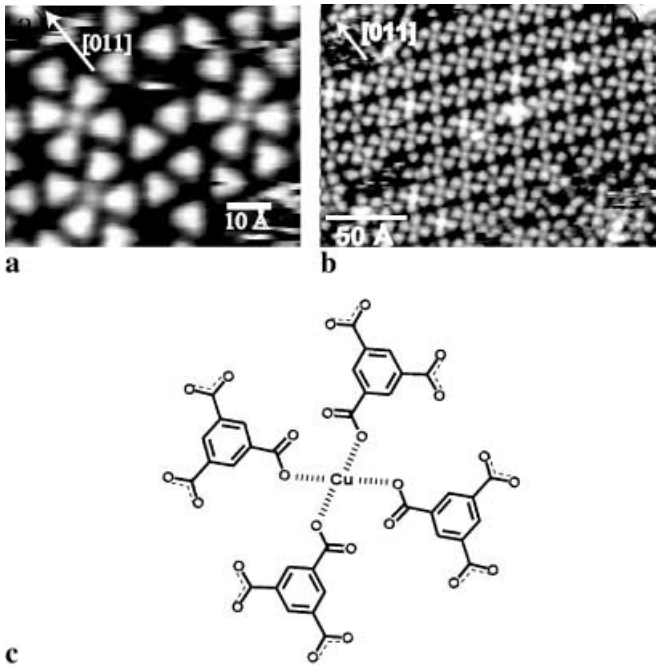

FIGURE 6 **a** STM topograph of TMA adsorbed on a Cu(100) surface at 300 K. The triangular shape reflects a flat-lying adsorption geometry. Cloverleaf-shaped arrangements of four TMA molecules with a central protrusion represent $Cu(TMA)_4$ coordination compounds. **b** Regular ordering of the complexes close to saturation coverage. **c** Model for the $Cu(TMA)_4$ compound with a Cu adatom coordinated by four carboxylate ligands. In agreement with the STM image, the TMA triangles do not point straight to the central site, indicating unidentate coordination of the central Cu. Adapted from [47]

that in theoretical calculations, carboxylate formation at surfaces with Cu–O distances of up to 2.6 Å and appreciable chemical bonding was found [50]). The Cu–O distance relaxation is attributed to the role of the substrate atomic lattice [47]. Moreover, the nature of the coordination bond itself is expected to be modified in the presence of the electrons from the Cu conduction band, which may account effectively even for substrate-mediated interactions. The square shape of the $Cu(TMA)_4$ configuration with its fourfold coordination is characteristic of Cu(II) complexes [51, 52]. Thus the cloverleaf arrangement per se should be considered formally as a $(Cu(II)(TMA)_4)^{10-}$ ion. However, the charge on both the Cu adatoms and the adsorbed TMA molecules is strongly affected by the presence of the electrons of the metal surface, which effectively screen any charged adsorbate. That is to say, an isolated deprotonated TMA molecule at the surface should not be considered as $(TMA_{ad})^{3-}$, but rather as a neutral TMA/Cu(001) complex. As an important consequence, the oxidation state of the central Cu atoms in the $Cu(TMA)_4$ configuration cannot be determined unambiguously. This contrasts with the situation encountered with isolated compounds in three dimensions, where the charge is usually balanced by counterions.

It is impossible to fabricate extended 1-D or 2-D networks where more than one carboxylate ligand per TMA participates in coordination-bond formation. This is again associated with the influence of the substrate atomic lattice, which pins the positioning and orientation of the reactive species at the surface. However, a second compound could be identified close to saturation of the TMA monolayer, where two Cu atoms are bound by six TMAs. An analysis of corresponding STM data [47] revealed that with this $Cu_2(TMA)_6$ configuration, four unidentate and two *syn syn* coordination bonds were present. In order to obtain quantitative information on the lifetime and formation of the compounds, measurements at small concentrations were undertaken, where both Cu adatoms and individual TMA molecules are highly mobile at the surface and elude direct observation. However, single or small groups of compounds could be readily resolved, i.e. the $Cu(TMA)_4$ configuration was stationary and could be imaged until it eventually dissociated. From an analysis of STM sequences recorded at room temperature with high scanning velocities, the average lifetime of an isolated cloverleaf was determined to be 34 ± 5 s. In a similar way, dissociation rates at reduced temperatures have been determined. As a result, the energy barrier for dissociation of the coordination compound (E_d) could be determined to be $E_d = 0.31 \pm 0.08$ eV [47]. With the present system, this energy is a convolution from the contributions associated with coordination bond formation and the repositioning of the involved elements.

5 Conclusions

The data presented demonstrate that supramolecular architectures and nanostructures at surfaces can be scrutinized at the single-molecule level by means of temperature-controlled STM. Assemblies stabilized by both hydrogen-bonding and metal–ligand interactions were addressed. It is suggested that systematic investigations may lead to a comprehensive rationale for deliberate construction of complex supramolecular aggregates and the positioning of functional units in specific geometries at suitable substrates. This approach is believed to be useful in the search for molecule-based nanoscale devices.

REFERENCES

1 F. Vögtle: *Supramolecular Chemistry* (Wiley, New York 1991)
2 J.M. Lehn: *Supramolecular Chemistry, Concepts and Perspectives* (VCH, Weinheim 1995)
3 J.L. Atwood, J.E.D. Davies, D.D. MacNicol, F. Vögtle, J.M. Lehn (Eds.): *Comprehensive Supramolecular Chemistry* (Pergamon, New York 1996)
4 J.S. Lindsey: New J. Chem. **15**, 153 (1991)
5 G.M. Whitesides, J.P. Mathias, C.T. Seto: Science **154**, 1312 (1991)
6 D. Philp, J.F. Stoddart: Angew. Chem. Int. Ed. **35**, 1154 (1996)
7 T. Kawai, H. Tanaka, T. Nakagawa: Surf. Sci. **386**, 124 (1997)
8 M. Böhringer, K. Morgenstern, W.D. Schneider, R. Berndt, F. Mauri, A.D. Vita, R. Car: Phys. Rev. Lett. **83**, 324 (1999)
9 M.O. Lorenzo, C.J. Baddeley, C. Muryn, R. Raval: Nature **404**, 376 (2000)
10 M. Furukawa, H. Tanaka, K. Sugiara, Y. Sakata, T. Kawai: Surf. Sci. **445**, L58 (2000)
11 J.V. Barth, J. Weckesser, C. Cai, P. Günter, L. Bürgi, O. Jeandupeux, K. Kern: Angew. Chem. Int. Ed. **39**, 1230 (2000)
12 L.A.M.M. Barbosa, P. Sautet: J. Am. Chem. Soc. **123**, 6639 (2001)
13 J. Weckesser, A.D. Vita, J.V. Barth, C. Cai, K. Kern: Phys. Rev. Lett. **87**, 096101 (2001)
14 T. Yokoyama, S. Yokoyama, T. Kamikado, Y. Okuno, S. Mashiko: Nature **413**, 619 (2001)
15 J.K. Gimzewski, C. Joachim: Science **283**, 1683 (1999)
16 C. Joachim, J.K. Gimzewski, A. Aviram: Nature **408**, 541 (2000)
17 G.A. Jeffrey, W. Saenger: *Hydrogen Bonding in Biological Systems* (Springer, Berlin 1991)
18 G.A. Jeffrey: *An Introduction to Hydrogen Bonding* (Oxford Univ. Press, New York 1997)
19 L.J. Prins, D.N. Reinhoudt, P. Timmerman: Angew. Chem. Int. Ed. Eng. **40**, 2382 (2001)
20 T. Steiner: Angew. Chem. Int. Ed. **41**, 48 (2002)
21 A. Werner: Z. Anorg. Chem. **3**, 267 (1893)
22 G. Wilkinson, R.D. Gillard, J.A. McCleverty (Eds.): *Comprehensive Coordination Chemistry* (Pergamon, Oxford 1987
23 J.P. Sauvage (Ed.): *Transition Metals in Supramolecular Chemistry,* (Wiley, Chichester 1999) p. 619
24 B.J. Holiday, C.A. Mirkin: Angew. Chem. Int. Ed. **40**, 2022 (2002)
25 A. Semenov, J.P. Spatz, M. Möller, J.M. Lehn, B. Sell, D. Schubert, C.H. Weidl, U.S. Schubert: Angew. Chem. Int. Ed. **38**, 2547 (1999)
26 H.H. Limbach, J. Manz (Eds.): *Hydrogen Transfer: Experiment and Theory*; Ber. Bunsenges. Phys. Chem. **102**, 289 (1998)
27 C. Cai et al.: Adv. Mater. **11**, 745 (1999)
28 C. Cai, J. Weckesser, J.V. Barth, B. Müller, Y. Tao, M.M. Bösch, C. Bosshard, P. Günter: Adv. Mater. **11**, 750 (1999)
29 C. Cai et al.: In: *Anisotropic Materials – Approaches to Polar Order*, ed. by R. Glaser, P. Kaszynski (ACS Symp. Series, 2001) p. 34
30 F.H. Herbstein: In: *Comprehensive Supramolecular Chemistry*, ed. by J.E.D.J.L. Atwood, D.D. MacNicol, F. Vögtle, J.M. Lehn (Pergamon, New York 1996) p. 61
31 S.V. Kolotuchin, P.A. Thiessen, E.E. Fenlon, S.R. Wilson, C.J. Loweth, S.C. Zimmerman: Chem. Eur. J. **5**, 2537 (1999)
32 F.H. Herbstein: Top. Curr. Chem. **140**, 107 (1987)
33 S. Chatterjee, V.R. Pedireddi, A. Ranganathan, C.N.R. Rao: J. Mol. Struct. **520**, 107 (2000)
34 O. Jeandupeux, L. Bürgi, A. Hirstein, H. Brune, K. Kern: Phys. Rev. B **59**, 15926 (1999)
35 H. Brune, H. Röder, K. Bromann, K. Kern: Thin Sol. Films **264**, 230 (1995)
36 J. Weckesser, J.V. Barth, K. Kern: J. Chem. Phys. **110**, 5351 (1999)
37 J. Weckesser, J.V. Barth, C. Cai, B. Müller, K. Kern: Surf. Sci. **431**, 268 (1999)
38 J.V. Barth, J. Weckesser, G. Trimarchi, M. Vladimirova, A.D. Vita, C. Cai, H. Brune, P. Günter, K. Kern: J. Am. Chem. Soc. **124**, 7991 (2002)

39 M. Vladimirova, G. Trimarchi, A.D. Vita, A. Baldereschi, J. Weckesser, K. Kern, J.V. Barth: (2002), submitted
40 P. Sautet: Chem. Rev. **97**, 1097 (1997)
41 A. Dmitriev, N. Lin, J. Weckesser, J.V. Barth, K. Kern: J. Phys. Chem. B **106**, 6907 (2002)
42 F.H. Herbstein, M. Kapon, I. Maor, M. Reisner: Acta Cryst. B **37**, 136 (1981)
43 D.J. Duchamp, R.E. Marsh: Acta Cryst. B **25**, 5 (1969)
44 C.C. Perry, S. Haq, B.G. Frederick, N.V. Richardson: Surf. Sci. **409**, 512 (1998)
45 M. Giesen: Surf. Sci. **442**, 543 (1999)
46 Q. Chen, C.C. Perry, B.G. Frederik, P.W. Murray, S. Haq, N.V. Richardson: Surf. Sci. **446**, 63 (2000)
47 N. Lin, A. Dmitriev, J. Weckesser, J.V. Barth, K. Kern: Angew. Chem. Int. Ed. (2002), in press
48 C. Oldham: In: *Comprehensive Coordination Chemistry*, ed. by G. Wilkinson, R.D. Gillard, J.A. McCleverty (Pergamon, Oxford 1987) p. 435
49 R.C. Mehrotra, R. Bohra: *Metal Carboxylates* (Academic Press, London 1983)
50 M. Sambi, G. Granozzi, M. Casarin, G.A. Rizzi, A. Vittadini, L.S. Caputi, G. Chiarello: Surf. Sci. **315**, 309 (1994)
51 A. Doyle, J. Felcman, M.T. do Prado Gambardella, C.N. Verani, M.L.B. Tristão: Polyhedron **19**, 2621 (2000)
52 P.R. Raithby, G.P. Shields, F.H. Allen, W.D.S. Motherwell: Acta Cryst. B **56**, 444 (2000)